Research Article

Synthesis of MnO$_2$ Microfiber with Secondary Nanostructure by Cotton Template

Huan-qin Wang, Ming-bo Zheng, Jin-hua Chen, Guang-bin Ji, and Jie-ming Cao

Nanomaterials Research Institute, College of Materials Science and Technology, Nanjing University of Aeronautics and Astronautics, Nanjing 210016, China

Correspondence should be addressed to Jie-ming Cao, jmcao@nuaa.edu.cn

Hierarchical MnO$_2$ microfibers were prepared by using cotton as the template and KMnO$_4$ as the precursor via an ultrasonic assistance route. The results of scanning electron microscope characterization showed that the concentration of KMnO$_4$ had a significant effect on the morphology of MnO$_2$ microfiber. At low concentration of KMnO$_4$, the microfiber was composed of MnO$_2$ nanorods with single crystal structure. With increasing the concentration of KMnO$_4$, the secondary nanostructure of MnO$_2$ microfibers had a transformation from nanorod to nanoparticle. The results of N$_2$ adsorption-desorption analysis indicated that MnO$_2$ microfibers had BET surface area of about 25 m^2/g. This synthesis provides a new way to control the secondary nanostructure of MnO$_2$ microfiber by adjusting the concentration of precursor. Furthermore, the mechanism for the replication was proposed and discussed.

1. Introduction

In recent years, many templates, such as mesoporous silica [1, 2], AAO [3–5], and surfactant micelle [6, 7], have been used for the preparation of nanostructured oxides. Biological materials have also been used as templates or scaffolds for the preparation of nanostructured oxides because of their interesting structures [8, 9]. In comparison with other templates, biological materials are "green" and easy to obtain. In the process of replication, the structure of biological materials provides a stable and controllable condition to guide the assembly of nanostructured oxides. The obtained nanostructured oxides can replicate the characteristic structures or even the functionalities of biological materials [10, 11]. Different species of biological materials, such as wood [12–14], filter paper [15, 16], and sisal [17], were used for the fabrication of various inorganic nanomaterials. In comparison with other kinds of plant fibers, the morphology of cotton fiber is more uniform.

In the past few years, MnO$_2$ nanomaterials have attracted considerable attention due to their potential applications in the areas of catalyst, ion-sieves, and electrode materials [18].

Recently, Zhu et al. prepared a series of manganese oxides via a "green" biotemplating method [19]. Herein, we fabricated MnO$_2$ microfibers with secondary nanostructure by using cotton as the template and KMnO$_4$ as the precursor. The effect of the concentration of KMnO$_4$ on the morphology of MnO$_2$ microfibers was studied and the possible formation mechanism was also discussed.

2. Experimental Section

Medical absorbent cotton was used as the template. It was pretreated before use. The cotton was immersed in 5 wt% HCl aqueous solution for 3 hours, washed with distilled water, and dried at 80°C in air. Then the sample was immersed in 6 wt% NaOH aqueous solution for 3 hours at 60°C, washed with distilled water, and dried at 80°C in air.

1.0 g of the pretreated cotton was dispersed in KMnO$_4$ aqueous solution in a beaker. The beaker was exposed to ultrasonic irradiation (100 W) for 6 hours. The sample was taken out, washed ten times with distilled water, and dried at 80°C in air. Then the sample was calcined at 500°C
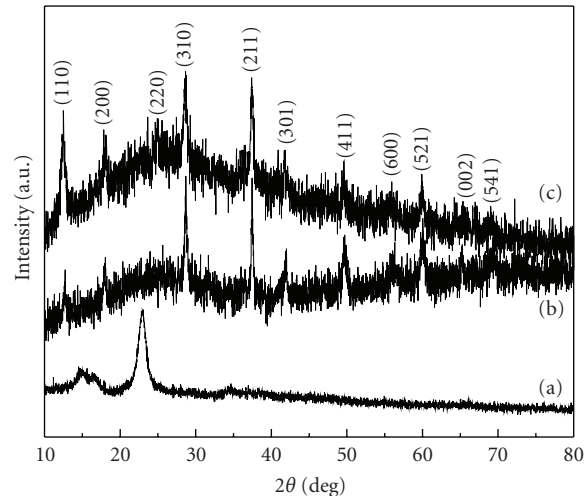
Figure 1: XRD patterns of the precursor/cotton of sample 1 (a), sample 1 (b), and sample 3 (c).

for 3 hours in air. Finally, the sample was washed with distilled water and alcohol to remove the byproduct, and then dried at $80°C$ in air. The concentrations of $KMnO_4$ aqueous solution were 5, 10, and 20 g/mL, respectively. The as-prepared samples were denoted as sample 1, sample 2, and sample 3, respectively. Furthermore, the sample without calcination process was denoted as the precursor/cotton.

The crystal structure of the sample was characterized by X-ray diffraction (XRD) (Bruker D8 advance). The morphology of the sample was examined by scanning electron microscopy (SEM Gemini LEO1530) and transmission electron microscopy (TEM JEOL JEM-2100). The N_2 adsorption-desorption analysis was measured on a Micromeritics ASAP 2010 instrument.

3. Results and Discussion

The XRD pattern of the precursor/cotton of sample 1 is shown in Figure 1a. Two peaks can be seen at about $15°$ and $23°$. It is difficult to judge the phase of the sample. Then the precursor/cotton was calcined to remove the cotton template. XRD patterns of sample 1 and sample 3 are shown in Figures 1(b), and 1(c), respectively. The results indicate that the samples are MnO_2 with a tetragonal structure (JCPDS 44-0141).

Figures 2(a) and 2(b) show the SEM images of the precursor/cotton of sample 1. Figures 2(c) and 2(d) shows the SEM images of the sample 1. Compared with the precursor/cotton sample, the obtained MnO_2 sample replicates the fiber structure of the cotton, but with some shrinkage in size. Figures 2(b) and 2(d) indicated that the surface morphology of MnO_2 microfiber is obviously different from the precursor/cotton sample. MnO_2 microfiber is composed of abundant nanorods. The TEM image (Figure 2(f)) also indicates that the microfiber is composed of nanorods. The corresponding selected-area electron diffraction (SAED) pattern (the inset in Figure 2(f)) indicates that the nanorods possess single crystal structure. The HRTEM images of the nanorods are shown in Figures 2(g) and 2(h). A layer

separation of about 0.69 nm can be observed, which is corresponding to the d value of the (110) planes of MnO_2.

Figure 3 shows the SEM images of sample 2 and sample 3. From the pictures, it can be seen that sample 2 is composed of nanoparticles and nanorods. Sample 3 is composed of nanoparticles. Therefore, it can be concluded that the secondary structure of the microfibers has a transformation from nanorod to nanoparticle with increasing the concentration of $KMnO_4$. In addition, the nanostructure of the microfibers becomes dense with increasing the concentration of $KMnO_4$.

The N_2 adsorption-desorption isotherms and the corresponding BJH pore-size distributions of MnO_2 microfibers are shown in Figure 4. All the samples have a sorption isotherm with a clear capillary condensation step in a relative pressure range of 0.9–1.0 (Figure 4(a)), implying the porous structure with large pore size. The porous structure was mainly produced from the stack of the nanomaterials. The BJH pore-size distributions indicate that all the samples possess large pore-size and broad pore distributions. The Brunauer-Emmett-Teller (BET) surface areas for sample 1, sample 2, and sample 3 are 24.8, 26.1, and 23.6 m^2/g, respectively. The pore volumes for sample 1, sample 2, and sample 3 are 0.12, 0.14, and 0.14 cm^3/g, respectively.

The formation mechanism of the samples is studied. The purpose of the pretreatment for the cotton is to remove the lignin and form $R-CH_2ONa$, which make MnO_4^- access the hierarchical pore channels more easily because of the resulting high porosity and the ionic environment [19]. The hydroxyl groups of the cotton facilitate the complexation of MnO_4^- ions with the cotton. In order to investigate the effect of ultrasonic irradiation, comparative experiment was performed. It is found that the precursor adsorbed on the cotton is very little if without the ultrasonic irradiation. The high-intensity ultrasound through water can lead to acoustic cavitation, which is the formation, growth, and violent collapse of gas microbubbles in the solution. The near adiabatic compression of the gas molecules inside the microbubbles in the liquid leads to a dramatic rise in the
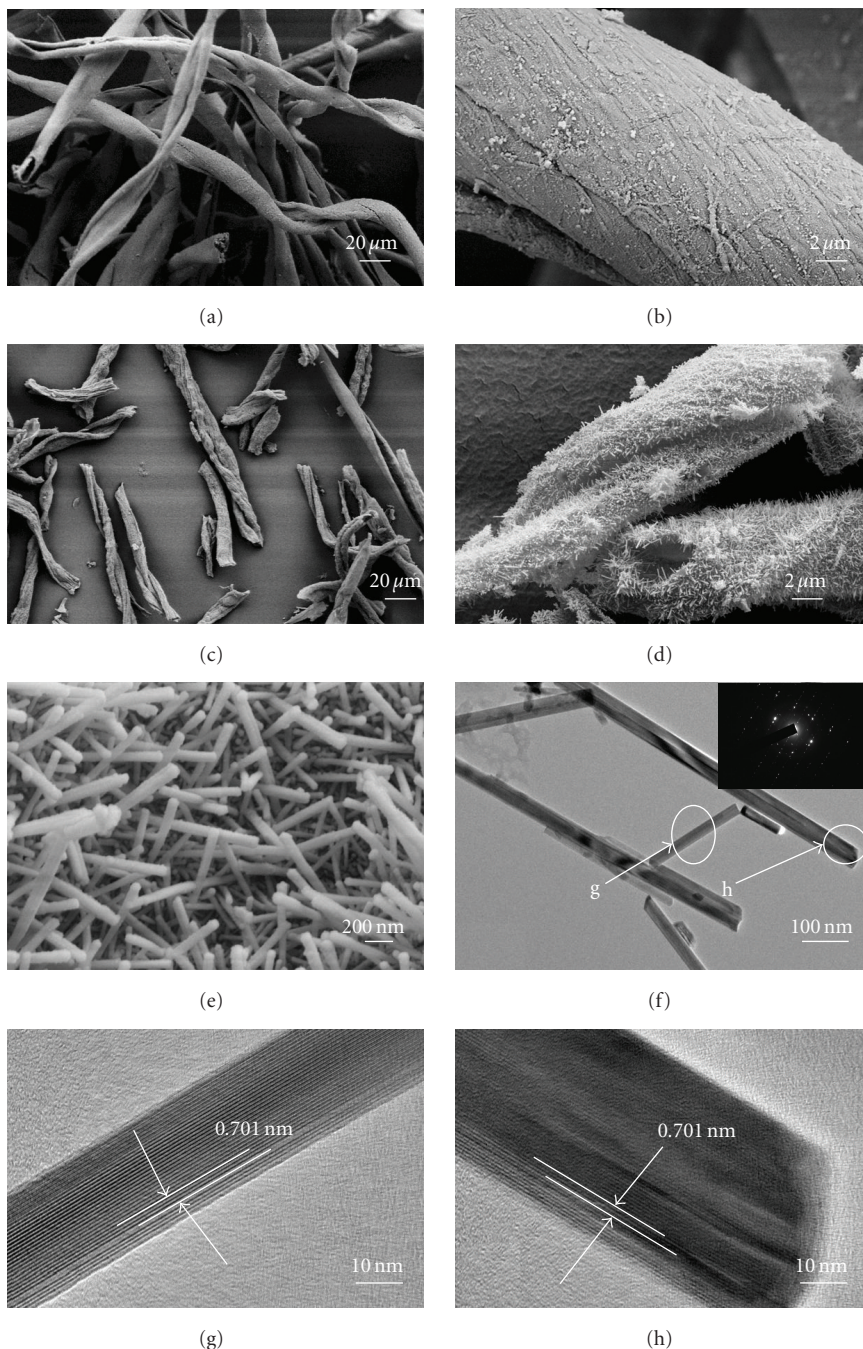
(a)

(b)

(c)

(d)

(e)

(f)

(g)

(h)

Figure 2: SEM images of the precursor/cotton of sample 1 (a), (b) and sample 1 (c)–(e) and TEM images of sample 1 (f)–(h); the inset in (f) is SAED pattern; the rectangle areas in panel (f) correspond to panels (g) and (h).

temperature and pressure within the bubbles [20], and this can have the effect of generating reactive free-radical species (MnO_4^- ions) in solution. The flow of solution made from the gas microbubbles leads to more MnO_4^- into the channels of cotton. The cotton fiber not only serves as the template for the formation of microfiber, but also provides the location for the nucleation and the growth of MnO_2 nanostructure during the heat treatment. Moreover, the hydroxyl groups of the cotton act as passivation contacts for the stabilization

of the nanoparticles formed inside the cotton. In addition, the concentration of the precursor plays an important role in the morphology of MnO_2 nanostructure. The SEM results (Figures 2(e) and 3(b)) indicated that the nanostructure becomes dense with increasing the concentration of $KMnO_4$. Thus, we think that the growth void of MnO_2 crystals determines the final morphology of the nanostructure. The nanorod structure can be obtained only when the growth void is enough.
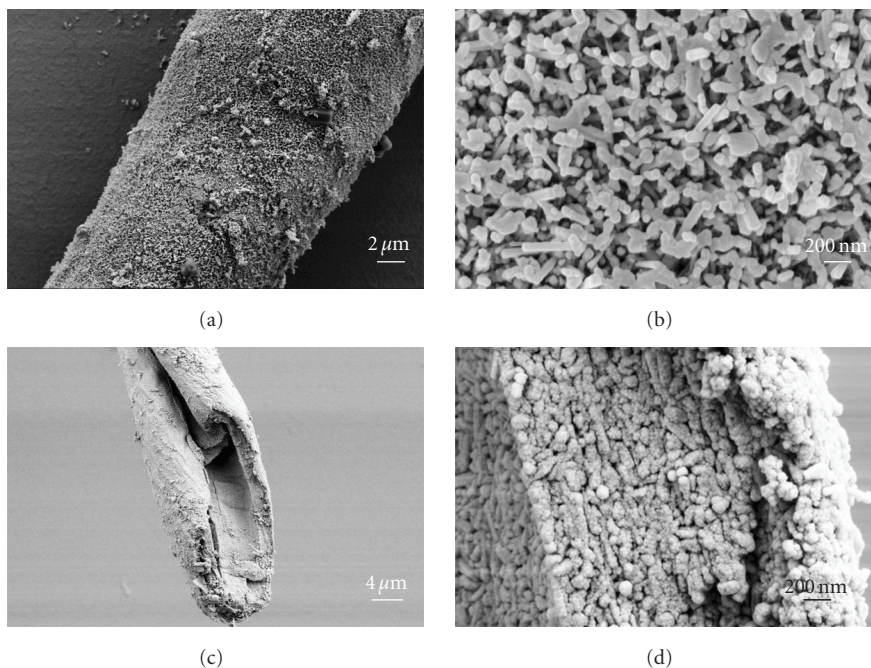
(a)

(b)

(c)

(d)

FIGURE 3: SEM images of sample 2 (a), (b) and sample 3 (c), (d).
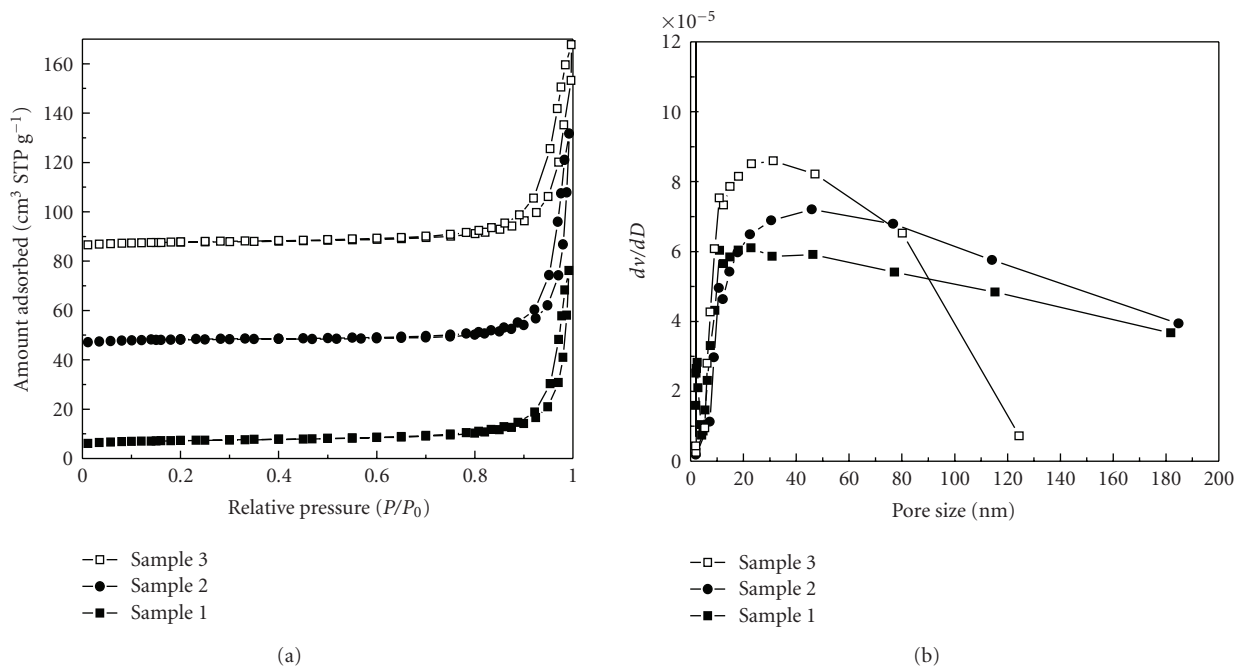

(a)

(b)

FIGURE 4: N_2 adsorption-desorption isotherms (a) and BJH pore-size distributions from adsorption branches (b) for the samples. The isotherms for sample 2 and sample 3 are offset vertically by 40 and 80 cm^3/g.

4. Conclusions

In conclusion, hierarchical MnO_2 microfibers with secondary nanostructure were successfully prepared by using cotton as the template and $KMnO_4$ as the precursor via an ultrasound route. The MnO2 microfibers with secondary nanostructure may be found to potential applications in the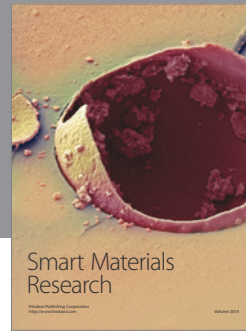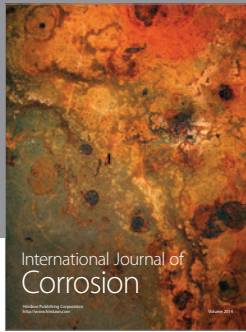 areas of catalyst, ion-sieve, and electrode material. It is expected that this biotemplating method can be extended to other metal oxide materials.

References

[1] M.-B. Zheng, J. Cao, S.-T. Liao, et al., "Preparation of mesoporous Co_3O_4 nanoparticles via solid-liquid route and effects of calcination temperature and textural parameters on their electrochemical capacitive behaviors," *Journal of Physical Chemistry C*, vol. 113, no. 9, pp. 3887–3894, 2009.

[2] P. Yang, D. Zhao, D. I. Margolese, B. F. Chmelka, and G. D. Stucky, "Block copolymer templating syntheses of mesoporous metal oxides with large ordering lengths and semicrystalline framework," *Chemistry of Materials*, vol. 11, no. 10, pp. 2813–2826, 1999.

[3] G. Ji, Z. Gong, W. Zhu, et al., "Simply synthesis of Co_3O_4 nanowire arrays using a solvent-free method," *Journal of Alloys and Compounds*, vol. 476, no. 1-2, pp. 579–583, 2009.

[4] W.-S. Chae, S.-W. Lee, and Y.-R. Kim, "Templating route to mesoporous nanocrystalline titania nanofibers," *Chemistry of Materials*, vol. 17, no. 12, pp. 3072–3074, 2005.

[5] X. Wang, X. Wang, W. Huang, P. J. Sebastian, and S. Gamboa, "Sol-gel template synthesis of highly ordered MnO_2 nanowire arrays," *Journal of Power Sources*, vol. 140, no. 1, pp. 211–215, 2005.

[6] G. Liu, B. Xie, D. Fu, Y. Wang, Q. Fu, and D. Wang, "Preparation of nearly monodisperse microcapsules with controlled morphology by in situ polymerization of a shell layer," *Journal of Materials Chemistry*, vol. 19, no. 36, pp. 6605–6609, 2009.

[7] Q. Zhou, X. Li, Y.-G. Li, B.-Z. Tian, D.-Y. Zhao, and Z.-Y. Jiang, "Synthesis and electrochemical properties of semicrystalline gyroidal mesoporous MnO_2," *Chinese Journal of Chemistry*, vol. 24, no. 7, pp. 835–839, 2006.

[8] S. Sotiropoulou, Y. Sierra-Sastre, S. S. Mark, and C. A. Batt, "Biotemplated nanostructured materials," *Chemistry of Materials*, vol. 20, no. 3, pp. 821–834, 2008.

[9] N. Ma, E. H. Sargent, and S. O. Kelley, "Biotemplated nanostructures: directed assembly of electronic and optical materials using nanoscale complementarity," *Journal of Materials Chemistry*, vol. 18, no. 9, pp. 954–964, 2008.

[10] D. Zhang and L. Qi, "Synthesis of mesoporous titania networks consisting of anatase nanowires by templating of bacterial cellulose membranes," *Chemical Communications*, no. 21, pp. 2735–2737, 2005.

[11] W. Zhang, D. Zhang, T. Fan, et al., "Novel photoanode structure templated from butterfly wing scales," *Chemistry of Materials*, vol. 21, no. 1, pp. 33–40, 2009.

[12] T. Fan, X. Li, J. Ding, D. Zhang, and Q. Guo, "Synthesis of biomorphic Al_2O_3 based on natural plant templates and assembly of Ag nanoparticles controlled within the nanopores," *Microporous and Mesoporous Materials*, vol. 108, no. 1–3, pp. 204–212, 2008.

[13] A. Dong, Y. Wang, Y. Tang, et al., "Zeolitic tissue through wood cell templating," *Advanced Materials*, vol. 14, no. 12, pp. 926–929, 2002.

[14] T. Ota, M. Imaeda, H. Takase, et al., "Porous titania ceramic prepared by mimicking silicified wood," *Journal of the American Ceramic Society*, vol. 83, no. 6, pp. 1521–1523, 2000.

[15] J. Huang, I. Ichinose, and T. Kunitake, "Biomolecular modification of hierarchical cellulose fibers through titania nanocoating," *Angewandte Chemie International Edition*, vol. 45, no. 18, pp. 2883–2886, 2006.

[16] J. Huang, N. Matsunaga, K. Shimanoe, N. Yamazoe, and T. Kunitake, "Nanotubular SnO_2 templated by cellulose fibers: synthesis and gas sensing," *Chemistry of Materials*, vol. 17, no. 13, pp. 3513–3518, 2005.

[17] J. He and T. Kunitake, "Preparation and thermal stability of gold nanoparticles in silk-templated porous filaments of titania and zirconia," *Chemistry of Materials*, vol. 16, no. 13, pp. 2656–2661, 2004.

[18] H. Zhang, G. Cao, Z. Wang, Y. Yang, Z. Shi, and Z. Gu, "Growth of manganese oxide nanoflowers on vertically-aligned carbon nanotube arrays for high-rate electrochemical capacitive energy storage," *Nano Letters*, vol. 8, no. 9, pp. 2664–2668, 2008.

[19] S. Zhu, D. Zhang, Z. Li, H. Furukawa, and Z. Chen, "Precision replication of hierarchical biological structures by metal oxides using a sonochemical method," *Langmuir*, vol. 24, no. 12, pp. 6292–6299, 2008.

[20] Y. Cao, J. Cao, J. Liu, M. Zheng, and K. Shen, "Sonochemical fabrication and photoluminescence properties of ordered mesopogpus carbon-tin oxide nanocomposites," *Chemistry Letters*, vol. 36, no. 2, pp. 254–255, 2007.